Biochimica et Biophysica Acta, 640 (1981) 207—222
© Elsevier/North-Holland Biomedical Press

BBA 79048

PHASE DIAGRAMS FOR IMPURE LIPID SYSTEMS

APPLICATION TO LIPID/ANAESTHETIC MIXTURES

F. DE VERTEUIL [a], D.A. PINK [b], E.B. VADAS [c,*] and M.J. ZUCKERMANN [a]

[a] *Department of Physics, McGill University, Montreal, Quebec,* [b] *Department of Physics, St. Francis Xavier University, Antigonish, Nova Scotia, and* [c] *Department of Biochemistry, McGill University, Montreal, Quebec (Canada)*

(Received June 17th, 1980)

Key words: Phase diagram; Anesthetic molecule; Cocaine derivative; Phospholipid; Fluidity; Transition temperature; (Lipid bilayer)

Summary

A physical model is presented to describe theoretically the temperature-dependent interactions of lipid bilayers with small molecules such as anaesthetics. Based on an earlier model, a triangular lattice in which each site is occupied by a single lipid chain is constructed and the small (anaesthetic) molecules are assumed to occupy interstitial sites in the centre of each lattice triangle. The phase characteristics of such lipid/anaesthetic mixtures are described in terms of the interaction parameters between lipid-lipid, lipid-anaesthetic and anaesthetic-anaesthetic molecules.

Depending on the chemical nature of the interacting species the following three models are formulated:

Model I. An interstitial model in which the only perturbation is in the head-group region of the bilayer and direct interactions between neighbouring anaesthetic molecules are taken into account.

Model II. Here, only hydrophobic interactions between anaesthetics and lipids are considered.

Model III. Both van der Waals' and coulombic interactions are taken into account.

Phase diagrams for the three models are obtained by numerical calculation over a wide range of interaction parameters. It is shown that in all three models, lateral phase separation takes place due to the presence of anaesthetics. The heat of transition, however, is found to be virtually independent of the anaesthetic concentration.

* Present address: Merck Frosst Laboratories, Kirkland, Quebec, Canada.

Introduction

Many studies dealing with the mode of action of anaesthetics focus on the change of fluidity of phospholipids upon interaction with the anaesthetic molecules [1—3]. In consequence, there is a considerable range of in vitro experiments which examine the fluidity of pure and mixed phospholipids as a function of anaesthetic concentration. The experimental methods include differential scanning calorimetry (DSC) [4,5], turbidity measurements [6], dilatometry [7], electron spin resonance (ESR) with spin labels such as TEMPO (2,2,6,6-tetramethylpiperidine-*N*-oxyl) [8,9], fluorescence spectroscopy [5,10] and nuclear magnetic resonance (NMR) [11—13]. The anaesthetic molecules used are both local anaesthetics such as synthetic cocaine derivatives (e.g., procaine, dibucaine, tetracaine), benzyl alcohol and long-chain alcohols as well as general anaesthetics (e.g., halothane, enflurane and other inhalation anaesthetics).

The main conclusion of the studies listed above is that at a sufficiently high concentration, most anaesthetics increase the fluidity of phospholipids in the liquid-crystalline or disordered state. There is, however, some controversy about the effect of anesthetics on lipid bilayers at low, clinical concentrations. Using ESR to study the effect of anaesthetics and pressure on lipid fluidity, Boggs et al. [14] concluded that clinical concentrations of a large variety of anaesthetics produced insignificant lipid fluidization. In contrast, Pelkofer and Sandhoff [15] recently reported an increase in membrane fluidity of synaptosomal plasma membranes even at clinical concentration of halothane as measured by fluorescence depolarization.

In general, an increase in lipid fluidity in the liquid-crystalline state is related to a decrease in the gel-to-liquid crystal transition temperature, T_c, with increasing anaesthetic concentration. Exceptions to this result are the *trans* saturated and unsaturated isomers of tetradecanol and hexadecanol which produce an increase in T_c of dimyristoyl phosphatidylcholine and distearoyl phosphatidylcholine bilayers with increasing anaesthetic concentration [16]. However, all anaesthetics appear to broaden the phase transition region in lipid bilayers.

In this paper, a general physical model is presented which describes quantitatively the temperature-dependent behaviour of impure lipid systems. In particular, we have chosen to use this model to evaluate the behaviour of lipid bilayers upon interaction with small anaesthetic molecules, thereby providing a framework for a systematic analysis of the above-cited experimental results. It is important to note at this point that the model applies to lipid/anaesthetic mixtures alone without taking into account the partition of anaesthetic between the lipid and the aqueous phase. However, real systems are composed of lipid/water mixtures; therefore, the problem of partition will be analyzed in the Discussion.

In the model, all the lipid chains lie on a triangular lattice. These lipid chains are all identical and fixed in position. The small molecules (anaesthetics) can only occupy interstitial sites and do not substitute for the lipid chains. If there are n (filled) lipid sites, then, from our choice of the interstitial site, there are $2n$ sites available for occupation by the small molecules. Suppose

$2nx$ ($x < 1$) small molecules now occupy interstitial sites and we allow them to interact with nearest neighbour lipid chains and with other neighbouring small molecules. Then, one possibility is to have a random distribution of the small molecules in the interstitial sites. The other possibility is for a phase separation to occur resulting in two lipid phases with different small molecule concentrations. It is important to realize that each small molecule is always surrounded by three lipid chains as it occupies an interstitial site, as shown schematically in Fig. 1a. Therefore, a phase containing small molecules only is never obtained. Also, the phase in which all interstitial sites are filled is a phase with n equivalent lipid chains and $2n$ anaesthetic molecules and it has a well defined gel-fluid phase transition. The lipid-anaesthetic interactions must be included since, obviously, no phase separation occurs without them. This model is conceptually different from that of Lee [17] which describes binary systems of two pure lipid components, A and B, each of which can exist in the pure A or B state.

Let us now examine the pertinent experimental data in some detail before applying the interstitial model to elucidate the observed phenomena. The DSC experiments of Mountcastle et al. [4] are of particular interest in this context. Here, the effects of the volatile general anaesthetics, halothane and enflurane, on dipalmitoyl phosphatidylcholine bilayers were examined. Both anaesthetics decreased T_c and broadened the phase transition region with increasing drug concentration. However, the heat of transition was found to be nearly independent of the anaesthetic concentration. Similar results were obtained by Papahadjopoulos et al. [5] in their extensive analysis of the effects of dibucaine dissolved in acidic phospholipid membranes using both DSC and fluorescent probes. It is also interesting to note that Cater et al. [18], in examining the effect of drugs on the phase transition temperature of dimyristoyl phosphatidylcholine and dipalmitoyl phosphatidylcholine, show that the heats of transition are effectively independent of drug concentration up to 50 mol% for both morphine derivatives and the tricyclic antidepressant, desipramine.

The analysis of DSC data using our model requires some knowledge of the location of the anaesthetic molecules in the bilayer. Shieh et al. [11] have deduced from high-resolution proton magnetic resonance (PMR) that volatile general anaesthetics act on the hydrophilic groups of the phospholipid molecules at physiological anaesthetic concentrations, and then diffuse into the hydrophobic region of the bilayer at high concentrations. They conclude that the general anaesthetics increase the motion of the positively charged head groups by weaking coulombic interactions. Other workers, however, conclude that hydrophobic molecules such as halothane may well exert their influence due to their ability to dissolve in the interior of the bilayer [14].

Recently, Turner and Oldfield [12] used deuteron magnetic resonance (^{2}H-NMR) to study the interactions of benzyl alcohol with dimyristoyl phosphatidylcholine bilayers. They find that the average orientational order parameter of the hydrocarbon chains decreases with increasing benzyl alcohol concentration, and the thickness of the bilayer is unchanged by the anaesthetic at physiological concentrations. They also show that benzyl alcohol causes a decrease in the quadrupole splitting and hence in the order parameter along

the hydrocarbon chains at higher concentrations. This is in contrast to the action of cholesterol in phospholipid bilayers [19], since cholesterol was found to cause an increase in bilayer thickness at comparable concentrations and a large increase in the order parameter along the hydrocarbon chain. Finally, some preliminary results using ^{2}H-NMR on egg phosphatidylcholine and phosphatidylcholine/phosphatidylserine mixtures containing procaine and tetracaine have been reported by Boulanger et al. [13]. In this case, both the hydrocarbon chains of the phospholipid molecules and the aromatic rings of the tetracaine were deuterated. The experimental data indicated that charged tetracaine molecules were attached to the bilayer at two different sites. At the first site, the tetracaine molecules are in the aqueous medium and seem to interact with the polar head groups of the lipids through their charged $N^+(CH_3)_2$ group and fast exchange with the aqueous medium takes place. At the second site, the tetracaine molecules are oriented parallel to the lipid hydrocarbon chains and hence their aromatic groups lie in the hydrophobic region of the bilayer. Only slow exchange with the aqueous medium may occur at this site.

Theory

The theory presented in this paper is based on the model of Caillé et al. [20] for lipid hydrocarbon chain dynamics in bilayers. This model has been used to analyse several properties of bilayers, including the enhanced diffusion of Na^+ out of dipalmitoyl phosphatidylcholine vesicles at T_c and the dimyristoyl phosphatidylcholine-dipalmitoyl phosphatidylcholine phase diagram in the region of 300 K. The theory accounts for the temperature dependence of the Raman intensities of the '1130 cm^{-1}' band of the hydrocarbon chain of

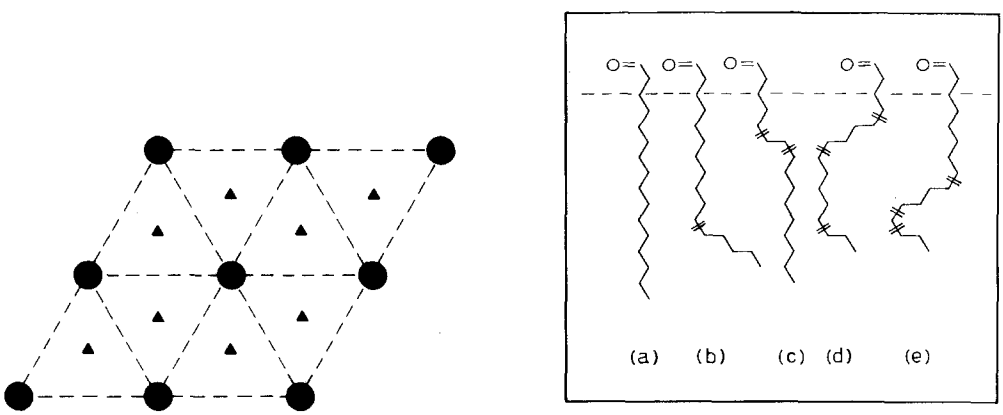

Fig. 1. (a) A schematic representation of the two-dimensional triangular lattice. The circles represent the sites of individual lipid hydrocarbon chains or substitutional impurities and the triangles represent interstitial sites for anaesthetic molecules. (b) The all-*trans* state and some intermediate states for a saturated hydrocarbon chain with 16 carbon atoms. The internal energies (E), areas (A) and degeneracies (D) are: (a) $E = 0$, $A = 20.4$ Å^2, $D = 1$; (b) $E = E_g$, $A = 23.54$ Å^2, $D = 2$; (c) kink, $E = 2E_g$, $A = 21.86$ Å^2, $D = 4$; (d) $E = 3E_g$, $A = 25.5$ Å^2, $D = 8$; (e) $E = 3E_g$, $A = 25.5$ Å^2, $D = 4$. Intermediate states do not have *gauche* rotations around the two bonds above the dashed line. E_g ($0.45 \cdot 10^{-13}$ erg) is the energy of a single *gauche* rotation (see Ref. 20).

pure bilayer lipids [21] and it has been used to examine the effects of intrinsic molecules such as cholesterol and proteins [22]. In particular, the model leads to an understanding of the rigidifying effect of cholesterol in fluid bilayers and its fluidizing effect on bilayers in the gel state.

The model assumes that each site of a triangular lattice is occupied by a single lipid chain as shown in Fig. 1a. Each lipid chain can exist in a number of configurations, some of which are shown in Fig. 1b; an all-*trans* state with zero internal energy which projects an area of 20.4 Å^2 onto a plane perpendicular to the long molecular axis, and a number of intermediate degenerate states which can be excited below the main transition temperature with little steric hindrance. All other physically realistic configurations may be included in one excited or melted state of high internal energy, E_M, high degeneracy, D_M, and 'cross-sectional' area of 34 Å^2. The internal energy and degeneracy of each state are related to the formation of two-fold degenerate *gauche* states and depend on the number of CH_2 groups per chain. Eight intermediate states, each of area less than 26 Å^2, were used by Pink et al. [21] to study the Raman data. The details of the excited state are unknown and its parameters must be determined from experiment. For pure dipalmitoyl phosphatidylcholine bilayers, E_M and D_M were found to be $2.74 \cdot 10^{-13}$ and $6 \cdot 3^{10}$ erg, respectively [22]. The hydrocarbon chains interact via a quadrupole-quadrupole interaction, J_0, due to London dispersion forces as described by Wulf [23]. The interaction between the polar head groups as modified by the surrounding water may be represented either by an effective lateral pressure, Π_e, first introducted by Marcelja [24] or by an effective coulombic interaction, K_0. Positive values of K_0 correspond to attractive coulombic interactions and negative values to repulsive coulombic interactions. Although the Hamiltonian function using Π_e has already been described in several publications [20—22], it is included here in the Appendix for the sake of completeness. The Appendix further includes a derivation of free energy in the molecular field approximation and some details of the numerical calculations. One of the salient points is that the symmetry break at the gel-fluid transition has been quantitatively taken into account. In the limit of a pure lipid system ($x_{\text{small molecule}} = 0$), the theory yields a sharp first-order phase transition, which is obtained by finding the temperature at which two separately calculated free energies for the gel and fluid phases are equal.

The next step is to model the site of interaction of the anaesthetic molecules in such a lattice. In this context, it should again be emphasized that cholesterol and anaesthetics have different effects on bilayers. For example, anaesthetics do not effectively alter the heat of transition, ΔH, at T_c whereas cholesterol progressively removes the phase transition. Moreover, cholesterol rigidifies neighbouring lipids in the fluid state whereas most anaesthetics tend to fluidize them. The behaviour of cholesterol in lipid bilayers is quite complex and the apparent changes in ΔH upon incorporation of cholesterol in the lipid bilayer are due to lateral phase separation into cholesterol-rich and phospholipid-rich regions [25,26]. Pink and Chapman [22] calculated the changes in ΔH and obtained a theoretical phase diagram for dimyristoyl phosphatidylcholine/cholesterol mixtures assuming that a cholesterol molecule can occupy a lattice site and they have theoretically predicted lateral

phase separation. Cholesterol is thus treated as a 'substitutional impurity' which interacts strongly via a quadrupole-quadrupole interaction with lipid chains in the all-*trans* state and very weakly with lipid chains in the excited state.

The insensitivity of the heat of transition to the presence of volatile anaesthetics in the bilayer therefore indicates that such small anaesthetic molecules in the bilayer cannot be considered as 'substitutional impurities' in the triangular lattice model. Hence, we place small anaesthetic molecules at interstitial sites in the centre of each lattice triangle in our model, allowing one anaesthetic site for every two lipid chains (see Fig. 1a). Any change in the coulombic interaction due to the anaesthetics is modelled by allowing the interaction, K_0, between charges on nearest neighbour lattice sites to be altered to $K_0 + K_1$, if an anaesthetic site is occupied in a triangle having both sites as vertices. Here, K_1 can be either positive or negative. This allows either an increase or decrease in the interaction between neighbouring head groups due to the presence of small interstitial impurities. A complete description of this model requires the inclusion of a direct interaction, J_{AA}, between neighbouring anaesthetic molecules. Positive J_{AA} corresponds to an attractive interaction. We now define model I by the variable parameters K_1 and J_{AA}. The model also requires knowledge of the numerical values of K_0 and J_0. These have been previously determined for pure lipids [20].

Certain local anaesthetics such as dibucaine and tetracaine have hydrophobic groups (e.g., aromatic rings) which will interact directly with the hydrocarbon chains of the lipids via London dispersion forces if part or all of the molecule penetrates into the interior of the bilayer. Since the experiments of Papahadjopoulos et al. [5] indicate that the heat of transition is independent of dibucaine concentration, we may assume that local anaesthetics can also be considered to occupy interstitial sites in the triangular lattice model at low concentrations. The hydrophobic interactions can then be modelled by quadrupole-quadrupole interactions between the hydrophobic groups of the anaesthetics and flexible hydrocarbon chains. These can also be written in the form derived by Wulf [23]. Since the anaesthetics should interact differently with rigid and with fluid lipid chains, at least two interaction parameters J_{AG} and J_{AM} must be defined. J_{AG} describes the interaction between a lipid chain in the ground state in any of the eight intermediate states with an anaesthetic molecule and J_{AM} describes the same interaction for lipids in the excited or 'melted' state. We can now construct two further models:

(a) Model II. In this case, the interaction between the polar head groups is modelled by using the lateral surface pressure, Π_e (=30 dyne/cm), introduced by Marcelja [24]. In this model, electrostatic interactions in the surface of the bilayer are not taken into account explicitly, i.e., only hydrophobic interactions between the anaesthetic molecules and the lipid chains are considered. Model II then is an interstitial model defined by the variables, J_{AG}, J_{AM} and J_{AA}, while the numerical values of Π_e and J_0 are known. In general, Π_e can be replaced by $\Pi_e + \Pi_e' y$, where y is the fraction of interstitial sites occupied by anaesthetic molecules and Π_e' is the change in latent pressure per anaesthetic molecule.

(b) Model III. When anaesthetic molecules are charged, e.g., dibucaine, both

electrostatic and London dispersion forces need to be taken into account. Model III is therefore an interstitial model which is described by the variables K_1, J_{AG}, J_{AM} and J_{AA} and the known parameters K_0 and J_0.

In order to calculate thermodynamic quantities and phase diagrams, the Hamiltonian functions describing models I–III were written in the molecular field (Bragg-Williams) approximation in terms of an order parameter, λ_W, for the hydrocarbon chains for all models and an order parameter, λ_p, for the polar head region for models I and II (see Appendix). A general expression for the free energy, F, is derived in terms of λ_W, λ_p and y is also presented in the Appendix. $F(\lambda_W, \lambda_p, y)$ is then minimised with respect to the order parameters and self-consistent expressions for λ_p and λ_W are derived. The expressions for F, λ_p and λ_W can now be used to calculate the thermodynamic quantities for a homogeneous mixture of lipids and anaesthetics. Let x be the mole fraction of anaesthetics for the interstitial model described above. Then x and y are related by the equation: $x = 2y/(1 + 2y)$.

The construction of phase diagrams for lipid/anaesthetic mixtures requires a free energy calculation for two homogeneous mixtures, each with different anaesthetic mole fractions, x_1 and x_2, and a fixed total mole fraction, x, such that $x_1 < x < x_2$ [20,22]. This requires four free energy terms which describe the two gel (G) and two fluid (F) phases having anaesthetic mole fractions of x_1 and x_2, respectively (see Appendix). x_1 and x_2 are varied at a fixed temperature, T, until a minimum in $F_{\alpha,\beta}(x_1, x_2)$ (α, β = F, G) is found. The values of x_1 and x_2 at the minimum value of $F_{\alpha,\beta}$ are the limiting mole fractions of a phase-separation region at temperature T providing $x_1 < x < x_2$. Phase diagrams were obtained by numerical calculation for models I–III over a wide range of interaction parameters. The results of these and other calculations are discussed in the next section.

Results and Discussion

The phase diagrams for lipid/anaesthetic mixtures found from numerical calculations for model I are shown in Figs. 2–4. The lipid was chosen to be dipalmitoyl phosphatidylcholine and in consequence, the values for J_0 and K_0 are those used to fit the model of Caille et al. [20] to experimental data: $J_0 = 0.73 \cdot 10^{-13}$ erg and $K_0 = 0.6125 \cdot 10^{-13}$ erg. Arbitrary values of the parameters K_1 and J_{AA} were chosen and varied systematically to cover a broad range of physical situations. Since there are insufficient experimental data available, it is somewhat difficult to match the theoretically obtained behaviour with physically realistic situations. This point will be elaborated below.

In our first calculation, the direct interaction between anaesthetics was taken to be attractive and weaker than the interaction J_0 between the lipid chains, i.e., $J_{AA} = 0.3 \cdot 10^{-13}$ erg. The interaction K_1 was chosen to have a negative sign and its magnitude was increased up to a value of $-0.55 \cdot 10^{-13}$ erg. This corresponds to a weakening of the interaction K_0 between polar head groups by the anaesthetic molecules. In this case, a narrow gel-fluid phase separation region was found in the vicinity of T_c for all values of K_1 which broadened as the magnitude of K_1 increased. The value of K_1 was then fixed at $-0.55 \cdot 10^{-13}$ erg in order to maintain bilayer integrity and J_{AA} was increased

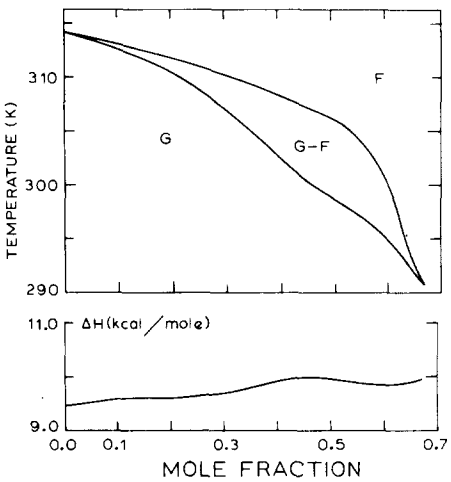

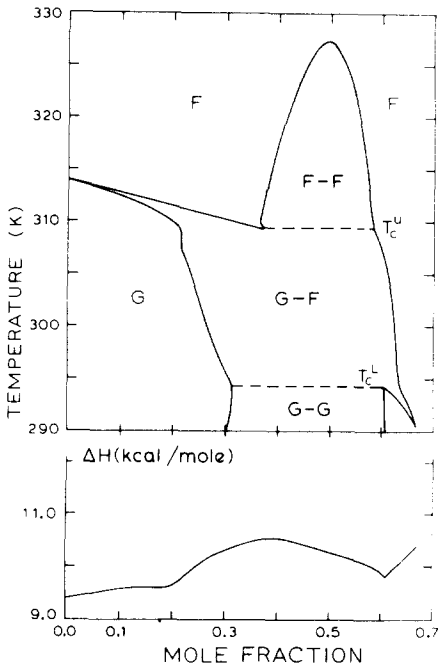

Fig. 2. (Top) Phase diagram near the gel-to-liquid crystal transition in a mixture of dipalmitoyl phosphatidylcholine and anaesthetic molecules described by model I. The parameters used (in units of 10^{-13} erg) are $J_0 = 0.734$, $K_0 = 0.6125$, $E_M = 2.78$, $J_{AA} = 0.45$, $K_1 = -0.55$. (Bottom) The heat of transition, ΔH, vs. mole fraction x, across the phase separation region.

Fig. 3. (Top) Phase diagram near the gel-to-liquid crystal transition in a mixture of dipalmitoyl phosphatidylcholine and anaesthetic molecules described by model I. The parameters used (in units of 10^{-13} erg) are $J_0 = 0.734$, $K_0 = 0.6125$, $E_M = 2.78$, $J_{AA} = 0.6$, $K_1 = -0.55$. T_c^u and T_c^L refer to the upper and lower main phase transition temperatures, respectively. (Bottom) The transition enthalpy, ΔH, vs. mole fraction, x, across the phase-separation region.

in magnitude. The resulting phase diagram is shown in Fig. 2. Here, the phase-separated region is very broad for higher anaesthetic concentrations ($0.2 < x < 0.6$) when $J_{AA} = 0.45 \cdot 10^{-13}$ erg. The nature of the phase diagram changes completely when J_{AA} is increased to $0.6 \cdot 10^{-13}$ erg. This is shown in Fig. 3. The broadened region of Fig. 2 becomes a bell-shaped curve with three different phase separated regions: gel-gel, gel-fluid and fluid-fluid. The phase diagram also exhibits a eutectic point and is similar to the phase diagram found by Pink and Chapman [22] for small substitutional molecules which interact strongly with rigid chains. The reason for the bell-shaped curve is that the interstitial impurities begin to form clusters at a given anaesthetic concentration for sufficiently large values of J_{AA}. This gives rise to fluid-fluid and gel-gel phase separation in the appropriate temperature range, since the interstitial impurities are always surrounded by lipid chains. The broad fluid-gel region beneath the bell-shaped curve occurs because the interstitial anaesthetic molecules fluidize the neighbouring lipid chains in the anaesthetic-rich phase, which therefore has a lower main transition temperature T_c^L. The phase with a lower anaesthetic concentration, however, has a high value T_c^u of T_c and therefore remains in the gel state to higher temperatures. When J_{AA} is increased

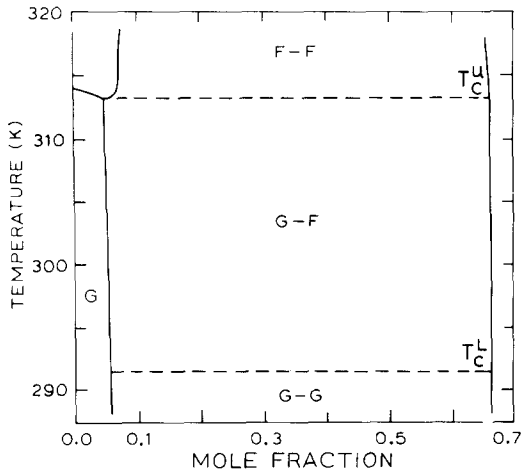

Fig. 4. The phase diagram near the gel-to-liquid crystal transition in a mixture of dipalmitoyl phosphatidylcholine and anaesthetic molecules described by model I. The parameters used (in units of 10^{-13} erg) are $J_0 = 0.734$, $K_0 = 0.6125$, $E_M = 2.78$, $J_{AA} = 1.0$, $K_1 = -0.55$. T_c^u and T_c^L refer to the upper and lower main phase transition temperatures, respectively.

to 10^{-13} erg, the attractive interaction between the anaesthetics dominates all other interactions. In this case, phase separation occurs for all but the lowest concentrations as shown in Fig. 4.

The calculated heat of transition only shows a small change as a function of anaesthetic mole fraction across the phase-separation region except in the bell-shaped portion (see Figs. 2—4). The enthalpy is a continuous function of temperature which increases sharply across the phase separation region when $J_{AA} = 0.6 \cdot 10^{-13}$ erg, $K_1 = -0.55 \cdot 10^{-13}$ erg and $x = 0.2$. This implies that the peak at T_c in the DSC measurements should broaden as a function of anaesthetic concentration. This is indeed the case for dipalmitoyl phosphatidylcholine/volatile anaesthetic systems as described by Mountcastle et al. [4]. This does not apply to the bell-shaped phase-separated region of Fig. 3 ($J_{AA} = 0.6 \cdot 10^{-13}$ erg), and to the phase-separated regions of Fig. 4 ($J_{AA} = 1 \cdot 10^{-13}$ erg). The heat of transition is now distributed between a sharp lower phase transition for the anaesthetic-rich phase at T_c^L and a sharp upper phase transition for the anaesthetic-deficient phase at T_c^u. Thus, there should be two separate peaks in the DSC data. In this context, it is interesting to note the shape of the heating curves obtained by Cater et al. [18] with dimyristoyl phosphatidylcholine and dipalmitoyl phosphatidylcholine in the presence of one of the morphine derivatives and amitriptyline. The model presented here may provide the explanation for the appearance of the two peaks in the DSC scans.

In model II, where the anaesthetic-lipid interactions are strictly hydrophobic, the phase diagrams are qualitatively the same as those obtained for model I. Again, the nature of the phase diagram depends on the magnitude of J_{AA}. We obtain typical 'solid solution' phase-separation diagrams. ($J_{AG} = 0.0$, $J_{AM} = 0.5 \cdot 10^{-13}$ erg and $J_{AA} = 0.45 \cdot 10^{-13}$ erg.) If $J_{AM} > J_{AG}$, inter-

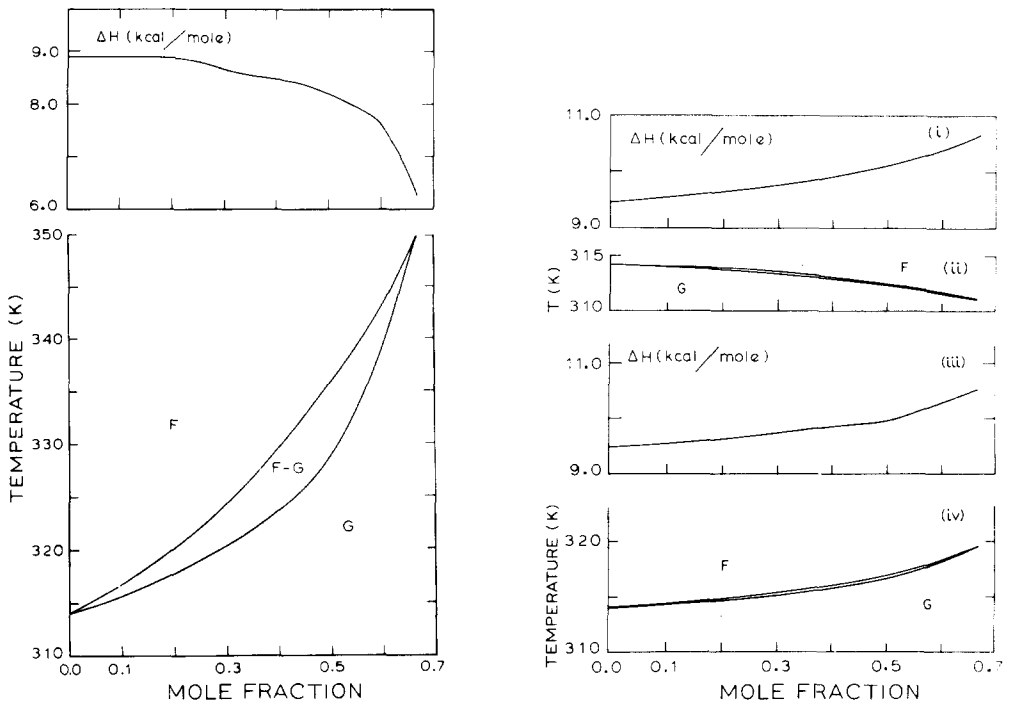

Fig. 5. (Top) Phase diagram near the gel-to-liquid crystal transition in a mixture of dipalmitoyl phosphatidylcholine and anaesthetic molecules described by model II. The parameters used (in units of 10^{-13} erg) are $J_0 = 0.734$, $E = 2.78$, $J_{AA} = 0.3$, $J_{AM} = 0.0$, $J_{AG} = 0.1$. The internal pressure $\Pi_e = 30$ dyne/cm. (Bottom) The heat of transition, ΔH, as a function of anaesthetic mol fraction, x, across the phase-separation region.

Fig. 6. The phase diagram and the corresponding heat of transition, ΔH, as a function of anaesthetic mol fraction, x, near the gel-to-liquid crystal transition in a mixture of dipalmitoyl phosphatidylcholine and anaesthetic molecules described by model III. The parameters used (in units of 10^{-13} erg) are $J_0 = 0.734$, $E_M = 2.78$, $J_{AG} = 0.0$, $J_{AM} = 0.45$. i and ii correspond to values $K_1 = 0.4$ and $J_{AA} = 0.45$; and iii and iv correspond to values $K_1 = 0.55$ and $J_{AA} = 0.3$, respectively.

stitial impurities prefer melted chains as neighbours resulting in a decrease in the value of T_c, corresponding to a negative K_1. Similarly, the case $J_{AG} > J_{AM}$ corresponds to positive K_1, and T_c increases with increasing anaesthetic concentration. The phase diagram resulting from such an increase in T_c is shown in Fig. 5 for $J_{AG} = 0.1 \cdot 10^{-13}$ erg and $J_{AA} = 0.3 \cdot 10^{-13}$ erg.

Lastly, model III is of interest when the coulombic interaction, K_1, and the hydrophobic interaction between the anaesthetics and the lipid chains have opposite effects on T_c, e.g., when $K_1 > 0$ and $J_{AG} < J_{AM}$. The phase-separation region may then become much narrower because of the competition between the two types of interaction. This is shown in Fig. 6a for $K_1 = 0.55 \cdot 10^{-13}$ erg, $J_{AA} = 0.3 \cdot 10^{-13}$ erg, $J_{AG} = 0.0$, and $J_{AM} = 0.3 \cdot 10^{-13}$ erg and in Fig. 6b for $K_1 = 0.4 \cdot 10^{-13}$ erg, $J_{AA} = 0.45 \cdot 10^{-13}$ erg, $J_{AG} = 0.0$ and $J_{AM} = 0.3 \cdot 10^{-13}$ erg. The heat of transition for models II and III is again weakly dependent on anaesthetic concentration at low values of J_{AA}.

These results theoretically confirm the extreme sensitivity of the bilayer to the presence of small molecules such as anaesthetics. Such molecules will

always cause lateral phase separations in the bilayer. When the anaesthetic molecules are 'interstitial', the phase separation has a solid solution behaviour (i.e., a fluid-gel phase separation in the vicinity of T_c) at low concentrations or when the direct intermolecular interactions J_{AA} are weak. If J_{AA} is attractive and increases in magnitude, the anaesthetic molecules tend to cluster. This results in broad fluid-fluid, fluid-gel and gel-gel phase separations. The existence of a solid solution phase separation explains the temperature broadening of the main phase transition region seen in the experiments listed in the Introduction. Furthermore, the insensitivity of the heat of transition to low anaesthetic concentrations evidenced both experimentally and in the calculations for models I and III implies that it is reasonable to treat the anaesthetic molecules as interstitial impurities.

It is now possible to correlate actual lipid-anaesthetic systems with each of the three models. Model I can be used to describe the behaviour of lipid/volatile anaesthetic mixtures at low anaesthetic mole fractions, where the anaesthetic molecules only perturb the polar head-group interactions. Model II can be related to systems such as lipid/benzyl alcohol mixtures. In this case, the polar head-group region of the lipid bilayer should be much less perturbed than the hydrocarbon chains provided that the benzene ring of the anaesthetic lies in the hydrophobic region of the bilayer. The experimental results of Turner and Oldfield [12] indicate that benzyl alcohol fluidizes the membrane which is manifested by a decreasing order parameter at each carbon atom of the hydrocarbon chains. This implies that $J_{AM} > J_{AG}$ for this system. Calculations of the order parameter as a function of position along the hydrocarbon chains using model II are in progress. Model III provides a description of lipid-local anaesthetic systems such as lipid/dibucaine or lipid/tetracaine mixtures where the anaesthetics are polarizable and the benzene rings lie in the hydrophobic regions of the bilayer. This situation corresponds to the second site found by Boulanger et al. [13] for tetracaine molecules in phospholipid bilayers, where the anaesthetic molecules are oriented parallel to the lipid hydrocarbon chains and the aromatic rings are located in the hydrocarbon interior of the bilayer.

In general, the bilayer interfaces with an aqueous medium in the polar head-group region, resulting in the partition of the anaesthetic molecules between the bilayer and the surrounding medium. For single-phase homogeneous bilayer/anaesthetic mixtures with a well defined main phase transition temperature, such partitioning implies that the anaesthetic mole fraction in the gel phase, x_G, is not equal to that in the fluid phase x_F. Such a partition effect has not been included in the formalism leading to the results described above and will now be theoretically analyzed for single-phase homogeneous mixtures.

Previous authors [3,17,27] neglect lipid-anaesthetic and direct anaesthetic-anaesthetic interactions and examine the change in T_c with anaesthetic concentrations using the solution thermodynamics. This theory gives the following well known expression for the change, ΔT_c, in T_c [3,17,27] at low anaesthetic mole fractions ($x_F, x_G << 1$):

$$\Delta T_c = \frac{-k_B T_{co}^2}{\Delta H_0} (x_F - x_G) \tag{1}$$

where T_{co} is the transition temperature and ΔH_0 is the heat of transition of the pure 'solvent' bilayer in the appropriate units. In Eqn. 1, the lipid-lipid interactions are the only interactions considered and are implicit in the parameters T_{co} and ΔH_0. In order to investigate the general case $x_G \neq x_F$, the number of anaesthetic molecules in the bilayer was treated as a variable and the anaesthetics were considered to be adsorbed molecules on the bilayer surface. An extra term representing the free energy for a single adsorbed anaesthetic molecule was therefore added to the free energy of model I. The new free energy term $F = F(\lambda_W, \lambda_p, N_L, y)$ is now minimised with respect to both the number of lipid chains, N_L, and the fraction of interstitial sites occupied by anaesthetic molecules, y. The lipid components of F can now be written as follows: $F_L^G(x_G, T)$ represents the free energy of the gel-phase lipid at a fixed anaesthetic mole fraction x_G and at temperature T and $F_L^F(x_F, T)$ is the corresponding quantity for the fluid-phase lipid. The expression for the main transition temperature T_c is now given by the condition:

$$F_L^G(x_G, T_c) = F_L^F(x_F, T_c) \tag{2}$$

Eqn. 2 reduces to Eqn. 1 if the anaesthetic-lipid and anaesthetic-anaesthetic interactions are neglected, i.e., $K_1 = J_{AA} = 0$.

Minimisation of the free energy F with respect to y gives an expression for the equilibrium value for y in terms of the partition functions q_A for a single adsorbed anaesthetic molecule and in terms of the parameters J_{AA}, K_1 and λ_p. When $K_1 = J_A = 0$ this expression reduces to the Langmuir isotherm if q_A is identified as $[C_E]k$, where $[C_E]$ is the concentration of anaesthetic molecules in mol/l in the aqueous medium in equilibrium with the bilayer surface and k is the rate constant for the binding reaction.

Preliminary results of numerical calculations using the expressions for F_L^G and F_L^F with $J_{AA} = 0$ and $K_1 < 0$ (i.e., decreasing polar head-group interaction) are shown in Table I. The parameters for dipalmitoyl phosphatidylcholine were used and x_F was taken to be 0.1. Table I shows that (i) the maximum decrease in the main transition temperature for $x_G = 0$ occurs when $K_1 = 0$ and (ii) ΔT_c decreases in magnitude with increasing values of K_1. Lee [17] points out that such a departure from the result of Eqn. 1 occurs for dipalmitoyl phosphatidylcholine/*n*-octanol mixtures and ascribes this departure to the existence of a phase-separated region near T_c. However, the results shown in Table I indicate that this behaviour can be explained by the inclu-

TABLE I

EFFECT OF INTERACTIONS AND ANAESTHETIC PARTITION ON THE TRANSITION TEMPERATURE

T_{f1} is the main transition temperature for an anaesthetic/dipalmitoyl phosphatidylcholine mixture with anaesthetic fraction $y_A^F = 0.05$, $y_A^G = 0$. F, fluid state; G, gel state. T_{f2} is the corresponding temperature for $y_A^F = y_A^G = 0.05$. The parameters for dipalmitoyl phosphatidylcholine were used with $K_0 = 0.6125 \cdot 10^{-13}$ erg and $J_{AA} = 0$.

K_1 (erg) ($\times 10^{-13}$)	0.0	−0.2	−0.4	−0.55	−0.61
T_{f1} (K)	309.9	311.8	313.6	315	315.6
T_{f2} (K)	314.0	313.55	313.3	313	312.9

sion of interactions of the required sign between the lipid and the anaesthetic molecules.

The phase diagram for any lipid/anaesthetic mixture must therefore be adjusted so as to include the partition effect just described. Detailed calculations will be presented in a future article. Preliminary calculations indicate that, although the partition effect will cause quantitative changes in the phase boundaries, the qualitative behaviour of the phase diagrams described above does not change.

Wu and McConnell [28] used spin labels to obtain phase diagrams for mixed phospholipid systems. In particular, they obtained a bell-shaped curve with one eutectic point for dielaidoyl phosphatidylcholine and dipalmitoyl phosphatidylethanolamine mixtures, which has the same qualitative behaviour as the phase diagram of Fig. 3. However, for dielaidoyl phosphatidylcholine/dipalmitoyl phosphatidylcholine mixtures, only a broad solid-solution phase diagram was found. This implies that this bell-shaped phase diagram is due to the strong interactions between the polar head groups of the dipalmitoyl phosphatidylethanolamine molecules. This is precisely the reason for the bell-shaped region of Fig. 3, i.e., strong attractive anaesthetic-anaesthetic interactions. The same formalism will therefore be used to study mixtures of charged and uncharged lipids with identical hydrocarbon chains, provided the impurities are now treated substitutionally.

Appendix

Theory of lipid/small molecule mixtures

Following Ref. 20, the Hamiltonian, H_{tot}, for lipid/small molecule mixtures used in this article is written as follows:

$$H_{tot} = H_L + H_{LM} + H_M \tag{A1}$$

H_L is the Hamiltonian for the lipid system and is given by:

$$H_L = H_{LW} + H_{LC} + H_{LO} \tag{A2}$$

H_{LO} is the Hamiltonian representing the nine-hydrocarbon chain configurations of Fig. 1b plus an internal lateral pressure Π_e. It is written:

$$H_{LO} = \sum_{i,n=0}^{9} (E_n + \Pi_e A_n) L_{ni}$$

L_{ni} is the projection operator for a hydrocarbon chain on the i-th site of a triangular lattice in the n-th configurational state. A_n is the cross-sectional area of the n-th state. H_{LW} is the anisotropic van der Waals' interaction between nearest neighbouring lipid chains and written in the notation of Pink and Chapman [22]:

$$H_{LW} = \frac{-J_0}{2} \sum_{\langle ij \rangle} \sum_{m,n=0}^{9} I_m^W I_n^W L_{mi} L_{nj} \tag{A3}$$

$\langle ij \rangle$ implies nearest neighbour lattice sites. J_0 is described in the text and I_n^W is an interaction parameter which depends on the directional order para-

meters of the C-C bonds in the n-th configurational chain state and the dependence of van der Waals' interaction on distance [20]. H_{LC} is the coulombic interaction between the polar head groups of the lipid molecules and is written:

$$H_{LC} = -(K_0 + K_1 y)/2 \sum_{\langle ij \rangle} \sum_{m,n=0}^{9} I_m^P I_n^P L_{mi} L_{nj} \tag{A4}$$

K_0, y and K_1 are described in the text and I_m^P is an interaction related to the distance dependence of the coulombic interaction [20]. H_M in Eqn. A1 is the Hamiltonian representing the direct interaction between small molecules on nearest neighbouring interstitial sites and is given by:

$$H_M = \frac{-J_{AA}}{2} \sum_{\langle \bar{i}\,\bar{j} \rangle} A_{\bar{i}} A_{\bar{j}} \tag{A5}$$

where $A_{\bar{j}}$ is the projection operator for a small molecule on the site $\bar{j}$ of the interstitial honeycomb lattice.

Finally, H_{LM} is the direct anisotropic van der Waals' interaction between nearest neighbour small molecules and lipid chain and can be written:

$$H_{LM} = -J_{AG} \sum_{\langle ij \rangle} \sum_{n=0}^{8} I_n^W A_{\bar{j}} L_{in} - J_{AM} \sum_{\langle \bar{i}j \rangle} I_9^W A_{\bar{j}} L_{9i} \tag{A6}$$

Eqns. A1—A6 give an expression for the total Hamiltonian of the system. The free energy $F(\lambda_W, \lambda_p, y)$ of the system in the molecular field approximation can be derived from Eqns. A1—A6 and is given by:

$$\frac{F(\lambda_W, \lambda_p, y)}{N} = -kT \ln Z_L + \tfrac{1}{2}(K_0 + K_1 y)\lambda_P^2 + \tfrac{1}{2} J_0 \lambda_W^2 \frac{-J_{AA} x^2}{2}$$

$$+ 2kT[y \ln y + (1-y) \ln(1-y)] \tag{A7}$$

where Z_L is the partition function for the lipid chains and is given by:

$$Z_L = \sum_{n=0}^{9} D_n \exp[-E_n^{MF}/k_B T] \tag{A8}$$

Here, D_n is the degeneracy of the n-th configurational state and E_n^{MF} is the average energy of the n-th state in the molecular field approximation given by:

$$E_n^{MF} = E_n + \Pi_e A_n - (K_0 + K_1 y) I_n^P \lambda_P - J_0 I_n^W \lambda_W - J_{AG} \lambda_{AW} \tag{A9}$$

$$\lambda_{P,W} = \left(\sum_{n=0}^{9} I_n^{P,W} D_n \exp[-E_n^{MF}/k_B T] \right) / Z_L \tag{A10}$$

Eqns. A8—A10 form self-consistent equations for λ_p and λ_W and must be solved numerically. λ_{AW} is given by:

$$\lambda_{AW} = \lambda_W + \left(\frac{J_{AM}}{J_{AG}} - 1 \right) I_9^W D_9 \exp[-E_9^{MF}/k_B T]/Z_L \tag{A11}$$

Finally, N is the number of lattice sites and y is defined by the relationship $\langle A_{\bar{i}} \rangle = y$. The last term on the right-hand side of Eqn. A7 is the entropy

of disorder for a random distribution of small molecules on the interstitial lattice.

Calculations were now performed using Eqns. A7—A11 in the following manner:

(a) In the absence of small molecules ($y = 0$) and $\Pi_e = 0$, the Hamiltonian and the free energy reduce to the original model of Caillé et al. [20] for a pure lipid bilayer with a sharp first-order phase transition. The transition temperature, T_c, is found numerically by solving the self-consistent Eqns. A8—A10 for different starting values of λ_W and λ_p (e.g., $\lambda_W = 1$ for the gel phase and $\lambda_W = 0$ for the fluid phase) at a fixed temperature T. The related values of the free energy are then calculated and are different in the region of the van der Waals' loop. The value of T_c is the value of T in the loop region when the two free energies are equal. The enthalpy of transition can then be calculated as well. This was the procedure used to obtain consistent values of E_9, J_0^M and K_0 for several phospholipids (see Ref. 22 for details) by fitting to experimental data.

(b) Models I—III are special cases of the Hamiltonian of Eqn. A1 and therefore the free energy of Eqn. A7 for a non-zero concentration of small molecules. In particular, Π_e and J_{AG} are both taken to be zero in model I and K_0 is given the value $0.6125 \cdot 10^{-13}$ erg. Model II is obtained when K_0 and K_1 are both zero and Π_e is chosen as 30 dyne/cm [20]. Since both coulombic interactions between the small molecules and the lipid chains are included in model III, only Π_e is taken to be zero.

The phase diagrams are calculated as indicated in the text. However, since we now have a binary system which may separate into two subphases, we must calculate four free energies, $F'_{\alpha,\beta}(x_1, x_2)$ (α, β = F, G) (two for each subphase) at a fixed temperature. The absolute minimum of these four free energies for all possible mole fractions x_1 and x_2 of the subphases must then be obtained. This enables us to find the actual mole fraction x_1^0 and x_2^0 for the subphases and the states of each subphase. If $x_1^0 = x_2^0$, then the system is homogeneous and therefore does not undergo phase separation.

Acknowledgements

We wish to express our gratitude to Ante Padjen, Rodney Biltonen, Joan Boggs, Myer Bloom, Jean Charvolin, Keith Miller, Don Patterson, Camille Sandorfy, Jim Sheats and Ian Smith for interesting discussions and, in some cases, availability of results prior to publication. One of us (M.J.Z.) wishes to thank Bernard Coqblin and the Faculté des Sciences, Université de Paris-Sud, for a visiting professorship in June 1979 and Anadi Bhattarcharjee of the same institute for his suggestion of surface adsorption. The research work reported in this paper was supported in part by the National Science and Engineering Council of Canada and the 'Ministere de l'Education' of the Province of Quebec. We wish to express our extreme gratitude to Betty Peterson and Irene Harrigan for typing the manuscript.

References

1 Trudell, J.R. (1977) Anaesthesiology 46, 5—10
2 Seeman, P. (1972) Pharmacol. Rev. 24, 583—655
3 Miller, J.C. and Miller, K.W. (1975) in Physiological and Pharmacological Biochemistry (Blashko, H.K.F., ed.), pp. 33—46, Butterworths, London, U.K.
4 Mountcastle, D.B., Biltonen, R.L. and Halsey, M.J. (1978) Proc. Natl. Acad. Sci. U.S.A. 75, 4906—4910
5 Papahadjopoulos, D., Jacobson, K., Poste, G. and Shepherd, G. (1975) Biochim. Biophys. Acta 394, 504—519
6 Veda, I., Tashiro, C. and Arakawa, K. (1977) Anaesthesiology 46, 327—332
7 MacDonald, A.G. (1978) Biochim. Biophys. Acta 507, 26—37
8 Hubbell, W.L., McConnell, M.H. and Metcalfe, J.C. (1969) Br. J. Pharmacol. 35, 374—375
9 Trudell, J.R., Payan, D.G., Chin, J.H. and Cohen, E.N. (1975) Proc. Natl. Acad. Sci. U.S.A. 72, 210—213
10 Vanderkooi, J.M., Landesberg, R., Selick, H., II and MacDonald, G.G. (1977) Biochim. Biophys. Acta 464, 1—16
11 Shieh, D.D., Ueda, I., Lin, H.-C., and Eyring, H. (1976) Proc. Natl. Acad. Sci. U.S.A. 73, 3999—4002
12 Turner, G.L. and Oldfield, E. (1978) Nature 277, 669—670
13 Boulanger, Y., Schreier, S. and Smith, I.C.P. (1979) Biophys. J. 25, 12a
14 Boggs, J.M., Yoong, T. and Hsia, J.C. (1976) Mol. Pharmacol. 12, 127—135
15 Pelkofer, R. and Sandhoff, K. (1980) J. Neurochem. 34, 988—992
16 Pringle, M.J. and Miller, K.W. (1979) Biochemistry 18, 3314—3320
17 Lee, A.G. (1977) Biochim. Biophys. Acta 472, 285—344
18 Cater, B.R., Chapman, D., Hawes, S.M. and Saville, J. (1974) Biochim. Biophys. Acta 303, 54—59
19 Chapman, D. (1973) in Biological Membranes (Chapman, D. and Wallach, D.F.H., eds.), Vol. 2, pp. 91—144, Academic Press, New York
20 Caillé, A., Pink, D.A., de Verteuil, F. and Zuckermann, M.J. (1980) Can. J. Phys. 58, 582—611
21 Pink, D.A., Green, T.J. and Chapman, D. (1980) Biochemistry 19, 349—356
22 Pink, D.A. and Chapman, D. (1979) Proc. Natl. Acad. Sci. U.S.A. 76, 1542—1546
23 Wulf, A. (1977) J. Chem. Phys. 67, 2254—2266
24 Marcelja, S. (1976) Biochim. Biophys. Acta 445, 1—7
25 Estep, T.N., Mountcastle, D.B., Biltonen, R.L. and Thompson, T.E. (1978) Biochemistry 17, 1984—1989
26 Mabrey, S., Mateo, P.L. and Sturtevant, J.M. (1978) Biochemistry 17, 2464—2468
27 Hill, M.W. (1978) Ann. N.Y. Acad. Sci. 1308, 101—110
28 Wu, S.H.-W. and McConnell, H.M. (1975) Biochemistry 14, 847—854